Hybrid Neural Sliding Mode Control of a DFIG Speed in Wind Turbines

Habib Benbouhenni
Laboratoire d'Automatique et d'Analyse des Systèmes (LAAS), Departement de Génie Électrique, Ecole Nationale Polytechnique d'Oran Maurice Audin, Oran, Algeria.
E-mail: habib0264@gmail.com

Received: August 2017 Revised: September 2017 Accepted: November 2017

ABSTRACT:
Wind energy (WG) generation industry has taken more concentration of fabrics. The WG promising renewable source of electrical energy generation for the future. This article applied neural network (NN) technique on the sliding mode command (SMC) of a 1.5 MW doubly-fed induction generator (DFIG) wind turbine (WT). In order to command the energy following between the stator of the DFIG and the grid, a proposed command design uses NN method is applied for implementing a neural command low to remove completely the chattering phenomenon on a traditional SMC strategy. The use of this technique provides very satisfactory performance for the DFIG command. The DFIG is tested in association with a WT. The simulation schemes were developed in Matlab/Simulink environment and the simulation results are presented and discussed for the whole system.

KEYWORDS: Doubly Fed Induction Generator, Sliding Mode Command, Neural Network, Chattering Phenomenon, Wind Turbine.

1. INTRODUCTION

The DFIG is one of the most popular generators in WTs [1]. The DFIG offers some advantages, such as the reduced inverter and output filter. Castes due to low rotor-and grid side energy transformation ratings (25%-30%) [2]. However, the DFIG has the distinction of having two three-phase windings in the rotor and stator [3]. Energy electrical inverter which encompasses back to back (AC-DC-AC) energy source converter a DC link capacitor. The rotor side inverter (RSC) has to command the stator reactive and stator active powers on the stator side. And the grid side inverter (GSC) is to command the DC bus tension and to command the power factor.

Many different structure and methods can be used for command of a power inverter. One of the most common command strategies is space vector modulation (SVM) technique in αβ reference frame which obtain stator reactive and stator active power command of DFIG machine separately. In this work, we proposed a novel method of SVM strategy based on calculates of minimum (min) and maximum (max) of three reference signals.

Since Direct Vector Control (DVC) with two proportional-integral (PI) regulators is the classical command scheme and the simple command used for DFIG based WTS [4]. In this command strategy, the decoupling between *q*-axis and *d*-axis stator current is achieved with feedforward compensation, and thus the DFIG model becomes less difficult and PI regulators can be used [4]. In the classical DVC command, reactive and active power can be directly controlled by using PWM (pulse width modulation) strategy. Nevertheless, a few disadvantages limit the use of these modulation strategies such as stator active and reactive powers ripples. In many research papers on vector command, these adverse effects are reduced by using the space vector modulation (SVM) method. However, the robustness of the command is sacrificed.

Since, the sliding mode command (SMC) technique, with is built on variable structure command (VSC) strategy [5]. The SMC is used for robust command of nonlinear systems. However, the SMC achieved simple command scheme and robust command by adding a discontinuous command signal across the sliding surface, satisfying the sliding condition [6]. On the other hand, the SMC has a disadvantage, which is the chattering phenomenon caused by the discontinuous command action [7]. To treat these difficulties, several modifications to the original SMC command low have been proposed.

Artificial neural network (ANN) is one of the most popular intelligent commands for industrial. ANN strategy, an exact mathematical model is not necessary and has many models; such an NN contains three layers: input layers, hidden layers and output layers [8].

On way to improve SMC, strategy performance is to combine it with NN to from a neuro-sliding mode controller (NSMC). The design of an NSMC in achieving reduced chattering, simple layers structure, and robustness against disturbances and nonlinearities.

In this work, two different commands schemes will be compared with each other. These two command schemes are SMC command with three-level SVM inverter (SMC-3L-SVM) and NSMC command with three-level NSVM technique (NSMC-3L-NSVM). The proposed commands scheme is described clearly and simulation results are reports to demonstrate its effectiveness. The proposed command schemes are implemented with Matlab/Simulink.

2. MODEL OF DFIG

A DFIG is used to produce energy power at constant frequency whatever wind and shaft speed conditions. We used the *dq* modelling of the DFIG in the Park reference frame [9, 10].

$$\begin{cases} V_{ds} = R_s I_{ds} + \dfrac{d}{dt}\psi_{ds} - \omega_s \psi_{qs} \\ V_{qs} = R_s I_{qs} + \dfrac{d}{dt}\psi_{qs} + \omega_s \psi_{ds} \\ V_{dr} = R_r I_{dr} + \dfrac{d}{dt}\psi_{dr} - \omega_r \psi_{qr} \\ V_{qr} = R_r I_{qr} + \dfrac{d}{dt}\psi_{qr} + \omega_r \psi_{dr} \end{cases} \quad (1)$$

Rotor and stator fluxes:

$$\begin{cases} \psi_{ds} = L_s I_{ds} + M I_{dr} \\ \psi_{qs} = L_s I_{qs} + M I_{qr} \\ \psi_{dr} = L_r I_{dr} + M I_{ds} \\ \psi_{qr} = L_r I_{qr} + M I_{qs} \end{cases} \quad (2)$$

The rotor and stator angular velocities are linked by the following equation:

$$w_s = w + w_r \quad (3)$$

The mechanical equation is:

$$T_e = T_r + J \cdot \frac{d\Omega}{dt} + f \cdot \Omega \quad (4)$$

The torque depends on *dq* current and flux:

$$T_e = p\frac{M}{L_s}(\psi_{ds}.I_{qr} - \psi_{qs}.I_{dr}) \quad (5)$$

3. THREE-LEVEL NSVM TECHNIQUE

In recent years, the space vector modulation (SVM) is the most popular types of modulation strategies. The SVM technique was originally developed as a vector approach to pulse width modulation strategy for three-phase converter [12, 13]. The principle of SVM inverter is that the command voltage vector is approximately calculated by using three adjacent vectors [14]. However, this strategy reduces the total harmonic distortion (THD) of current and gives 15 % more voltage output compared to pulse width modulation inverter. In addition, this strategy is difficult to implement. On the other hand, this strategy based on calculating of angle and sector. In this paper, we propose a new algorithm of three-level SVM based on calculating of maximum (max) and minimum (min) of three-phase voltages. However, the block diagram of the three-level SVM inverter is given by Fig. 1. This proposed modulation technique is a simple scheme and easy to implement compared to the classical SVM technique. This strategy based on the following steps:

- Calculates the minimum voltages (min (Va, Vb, Vc))
- Calculates the maximum voltages (max (Va, Vb, Vc))
- Add the maximum and minimum voltages (max (Va, Vb, Vc) + min (Va, Vb, Vc)).
- The last step is to compare step-3 waveforms with Vp ($V_{Triangle}$) & Vp_1, and generates the pulses for that switch presents in the three-phase voltage source converter circuit.

In order to improve the three-level SVM performances a complimentary use of the artificial neural networks (ANN) is proposed. ANN is part of the family of statistical learning techniques inspired by biological nervous system and are used to estimate and approximate functions that depends only on a large number of inputs [15]. ANNs are commonly used for processing and filtering signals, for estimating and predicting signals, or as stand-alone controllers [16]. However, the ANN controller contains three layers: input layers, hidden layers and output layers.

The principle of the three-level neural space vector modulation (NSVM) is similar to traditional three-level SVM inverter. The difference is using neural controllers to replace the hysteresis comparators. As shown in Fig. 2. This proposed modulation gives minimum powers ripple and reduced the total harmonic distortion of rotor current compared to classical SVM

inverter. This strategy is a simple scheme and easy to implement.

The hysteresis comparators are replaced by ANN controllers and this technique based on neural classification has the advantage of easy implementation and simplicity. On the other hand, the artificial neural networks controller's parameters for the hysteresis comparators are shown in Table 1.

Table 1. The ANN parameters for the hysteresis comparators.

Parameters	**value**
Number of neurones for input layer	1
Number of neurones for output layer	1
Layer number	1
First layer cell number	12
Second layer cell number	-
First layer activation function	Tansig
Second layer activation function	Purelin
Maximum iteration number	1000
Error limit	0
Training coefficient	0.9
Momentum coefficient	0.8

The internal structure of neural networks based hysteresis comparators is shown in Fig. 3. However, the ANN controller is composed of two layers, Layer 1(Fig. 4) and Layer 2 (Fig. 5).

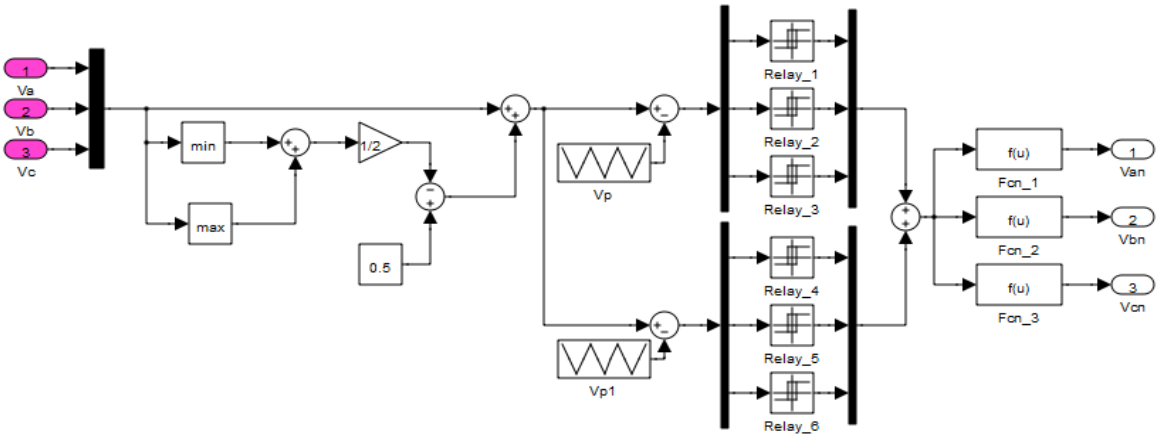

Fig.1. Block diagram of the three-level SVM inverter.

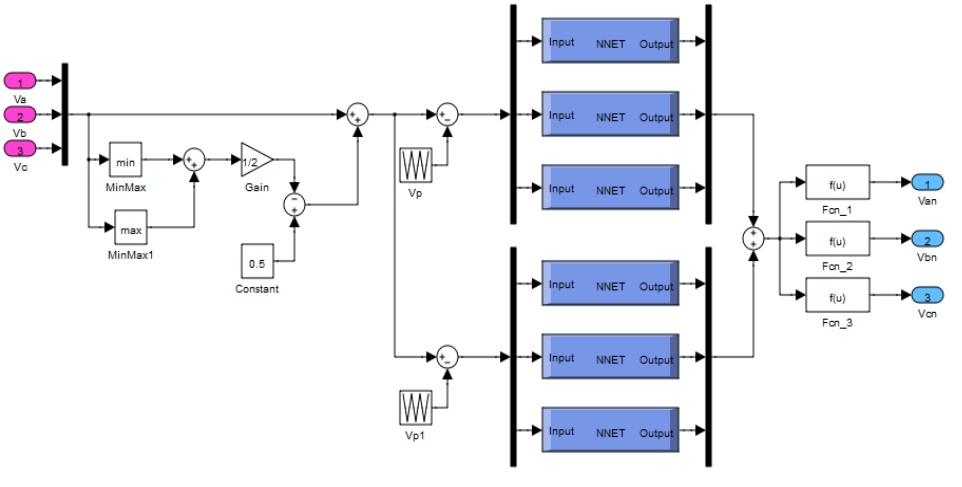

Fig. 2. Block diagram of the three-level NSVM.

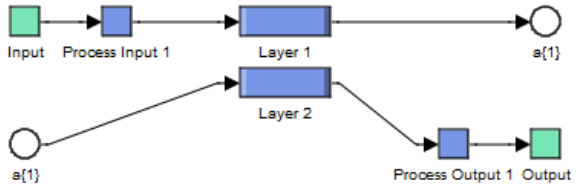

Fig. 3. Block diagram of the neural hysteresis comparators.

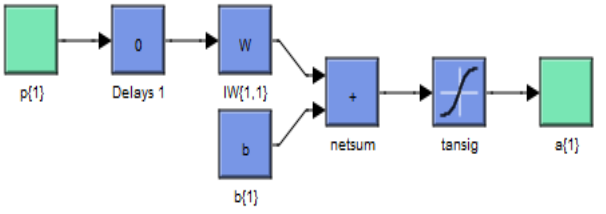

Fig. 4. Layer 1.

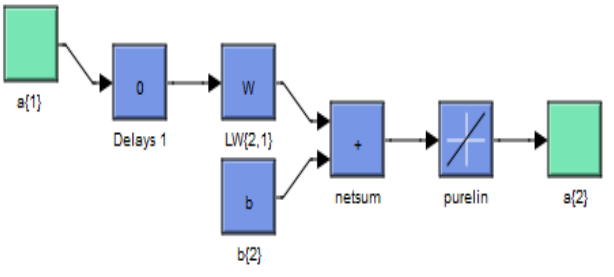

Fig. 5. Layer 2.

4. DIRECT VECTOR CONTROL

In this section, by choosing a reference frame linked to the stator flux, rotor currents will be related directly to the stator reactive and stator active energy. An adapted command of these currents will thus permit command the energy exchanged between the stator and the grid. If the stator flux is linked to the d-axis of the frame we have:

$$\psi_{ds} = \psi_s \quad \text{and} \quad \psi_{qs} = 0 \tag{7}$$

By neglecting Rs the stator voltage will be expressed by:

$$\begin{cases} V_{qs} = 0 \\ V_{ds} = \omega_s \psi_s \end{cases} \tag{8}$$

$$\begin{cases} I_{ds} = -\dfrac{M}{L_s} I_{dr} + \dfrac{\psi_s}{L_s} \\ I_{qs} = -\dfrac{M}{L_s} I_{qr} \end{cases} \tag{9}$$

The stator active and reactive powers are imposed by the direct component I_{dr} by**:**

$$\begin{cases} P_s = -\dfrac{3}{2}\dfrac{\omega_s \psi_s M}{L_s} I_{qr} \\ Q_s = -\dfrac{3}{2}\left(\dfrac{\omega_s \psi_s M}{L_s} I_{dr} - \dfrac{\omega_s {\psi_s}^2}{L_s} \right) \end{cases} \tag{10}$$

Stator flux can be expressed:

$$\psi_s = \frac{V_s}{w_s} \tag{11}$$

Where Vs : is the rms value of the grid voltage.

The rotor voltages can be expressed [17]:

$$\begin{cases} V_{dr} = R_r . I_{dr} + (L_r - \dfrac{M^2}{L_s}).s.I_{dr} - g.w_s.(L_r - \dfrac{M^2}{L_s}).I_{qr} \\ V_{qr} = R_r . I_{qr} + (L_r - \dfrac{M^2}{L_s}).s.I_{qr} + g.w_s.(L_r - \dfrac{M^2}{L_s}).I_{dr} + g.\dfrac{M.V_s}{L_s} \end{cases} \tag{12}$$

In steady state, the second derivate terms of the two equations in (12) are nil. We can thus write:

$$\begin{cases} V_{dr} = R_r . I_{dr} - g.w_s.(L_r - \dfrac{M^2}{L_s}).I_{qr} \\ V_{qr} = R_r . I_{qr} + g.w_s.(L_r - \dfrac{M^2}{L_s}).I_{dr} + g.\dfrac{M.V_s}{L_s} \end{cases} \tag{13}$$

The electromagnetic torque can then be expressed by:

$$T_e = -\frac{3}{2} p \frac{M}{L_s} I_{qr} \psi_{ds} \tag{14}$$

5. SLIDING MODE CONTROLLER (SMC)

The SMC method is developed from VSC to solve the disadvantages of there stylisme of nonlinear command systems [18]. The SMC is a strategy to adjust feedback by formerly defining a surface. The system which is controlled will be required to that surface, then the behaviour of the system solides to the desired balance point [19]. Since the robustness is the best advantage of an SMC, it has been widely employed to command nonlinear systems that have model uncertainty and external disturbance [20]. Fig. 3 represents the SMC control scheme of DFIG driven by a two-level SVM technique.

5.1. Design of The Sliding Mode Controllers

The article designs the following sliding mode, let:

$$\begin{cases} S_p = P_{s_{ref}} - P_s \\ S_q = Q_{s_{ref}} - Q_s \end{cases} \quad (15)$$

Where $P_{s\ ref}$ and $Q_{s\ ref}$ are the expected stator active and reactive power reference.

The first order derivate of (15), gives:

$$\begin{cases} \dot{S}_p = \dot{P}_{s_{ref}} - \dot{P}_s \\ \dot{S}_q = \dot{Q}_{s_{ref}} - \dot{Q}_s \end{cases} \quad (16)$$

Replacing the expression of the power by their expressions given in (10), the equations below are expressed:

$$\begin{cases} \dot{S}_p = \dot{P}_{s_{ref}} - \dfrac{V_s.M}{L_S}\dot{I}_{qr} + \dfrac{V_s^2}{R_s} - \dfrac{w_s^2\psi_s^2}{R_s} \\ \dot{S}_q = \dot{Q}_{s_{ref}} + \dfrac{V_s M}{L_s}\dot{I}_{dr} - \dfrac{w_s\psi_s^2}{L_s} \end{cases} \quad (17)$$

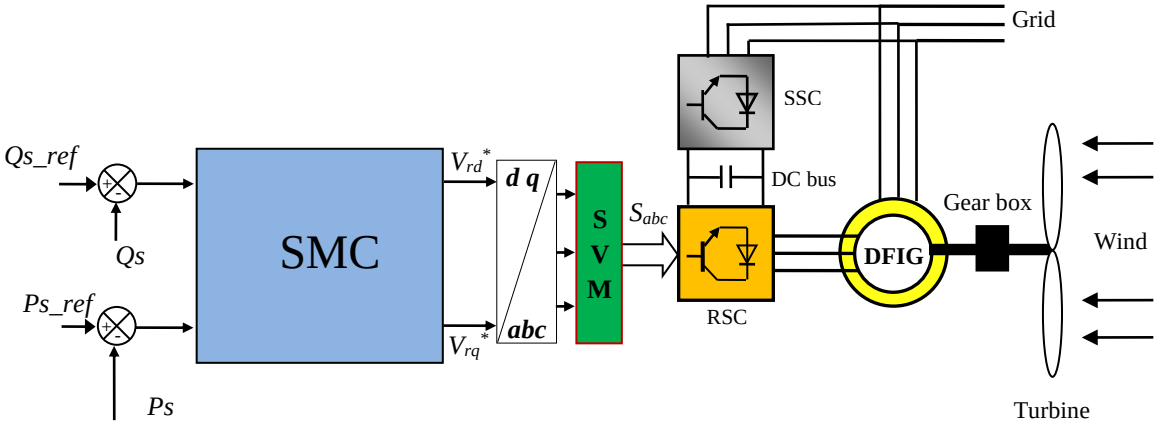

Fig. 6. SMC control of a DFIG using SVM strategy.

$$\begin{cases} V_{dr}^{eq} = R_r.I_{dr} - L_s\dfrac{(L_r - \frac{M^2}{L_s})}{M\,\psi_s\,w_s}\dot{Q}_{s_{ref}} - g.w_s.(L_r - \frac{M^2}{L_s}).I_{qr} + \dfrac{(L_r - \frac{M^2}{L_s})}{M}w_s \\ V_{qr}^{eq} = R_r.I_{qr} + \dfrac{L_s}{V_s M}\dot{P}_{s_{ref}} - g.w_s.(L_r - \frac{M^2}{L_s}).I_{dr} + g.\dfrac{M.V_s}{L_s} \end{cases} \quad (18)$$

To obtain good performances, dynamic and a commutation around the surface, the command vector is imposed as follows:

$$V_{dq} = V_{dq}^{eq} + V_{dq}^{n} \quad (19)$$

V_{dq}^{n} is the saturation function defined by :

$$V_{dq}^{n} = -K.sat(S_{dq}) \quad (20)$$

Where *K* determine the ability of overcoming the chattering

The SM will exist only if the following condition is met:

$$S.\dot{S} \prec 0 \quad (21)$$

It takes the current expression of $\dot{I}_{dr}$ and $\dot{I}_{qr}$, with the voltage equation (13) and taking into consideration the SMC in the steady state (S=0, $\dot{S} = 0$). The equivalent command vector V^{eq} can express by:

6. NEURO-SLIDING MODE CONTROL

The disadvantage of SMC is that the discontinuous command signal produces chattering. In order to improve the SMC command and eliminate the chattering phenomenon, we propose to use the ANN controllers. The Neuro-Sliding Mode Controllers (NSMC) is a modification of the SMC strategy, where the switching controller term sat(S(x)), has been replaced by NN regulator input as given below.

$$V_{dq}^{com} = V_{dq}^{eq} + V_{dq}^{Neural} \quad (22)$$

The proposed NSMC technique, which is designed to command the stator reactive and stator active powers of the DFIG machine, is shown in Fig. 7.

For the two proposed neuro-sliding mode controllers in Fig. 7, the structure of the NN with one linear input node, 8 neurons in the hidden layer and one neuron in the output layer, as shown in Fig. 8.

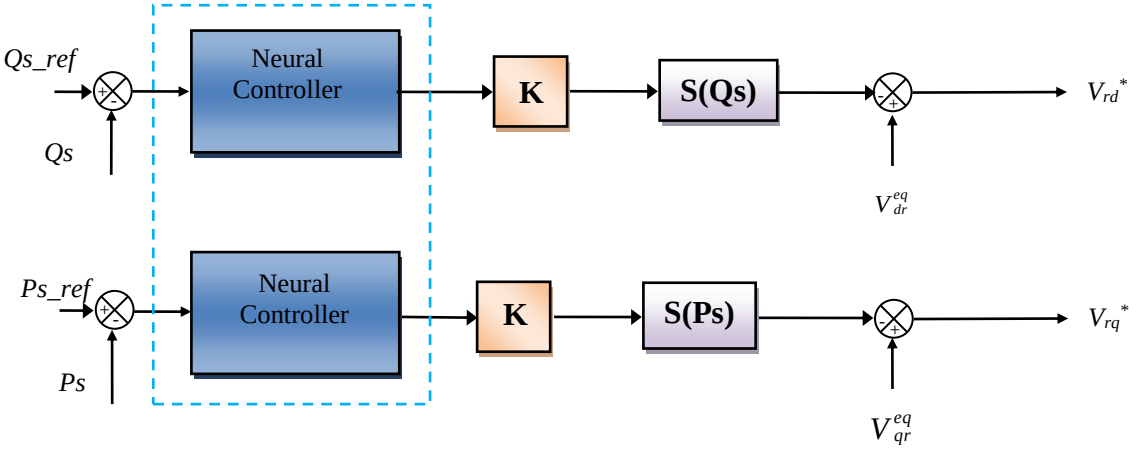

Fig. 7. Bloc diagram of the DFIG control with NSMC

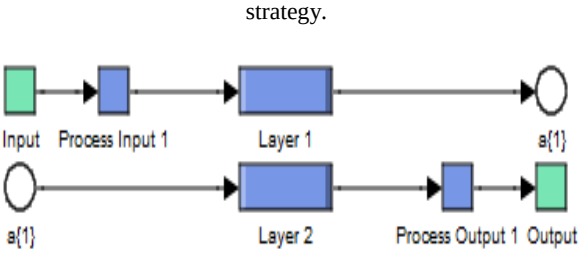

Fig. 8. Block diagram of the ANN controller for reactive and active powers.

The training used is that of the algorithm, Gradient descent with momentum & Adaptive LR. The number of the iteration count maximum 2000 with an iteration step of 50. The structure of Layer 1 and layer 2 is shown in Fig. 9 and Fig. 10 respectfully.

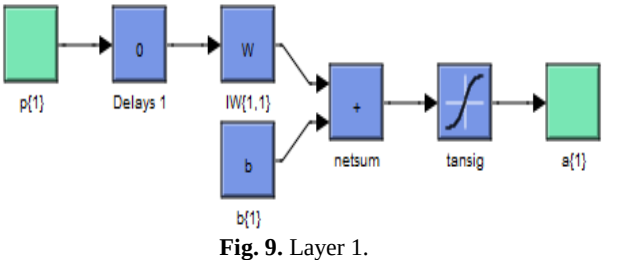

Fig. 9. Layer 1.

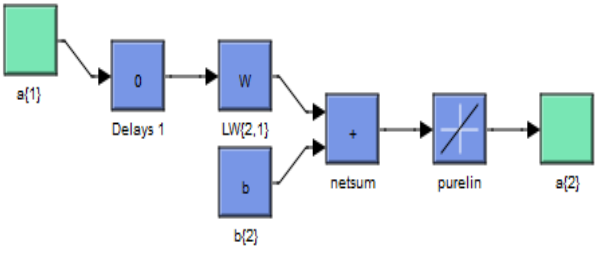

Fig. 10. Layer 2.

Fig. 11 shows the NSMC strategy of a doubly fed induction generator driven by a three-level NSVM technique.

7. SIMULATION RESULTS

In this part, simulations are investigated with a 1.5MW doubly fed induction generator connected to a 398V/50Hz grid. The machine parameters are presented in the Table 2. The proposed command schemes will be tested and compared in two different configurations: robustness against parameters variations and reference tracking.

Table 2. The DFIG parameters.

Parameters	Rated Value	Unity
P	1.5	MW
Vs	398/690	V
Fs	50	Hz
P	2	
Rs	0.012	Ω
Rr	0.021	Ω
Ls	0.0137	H
Lr	0.0136	H
M	0.0135	H
J	1000	Kg m^2
f	0.0024	Nm/s

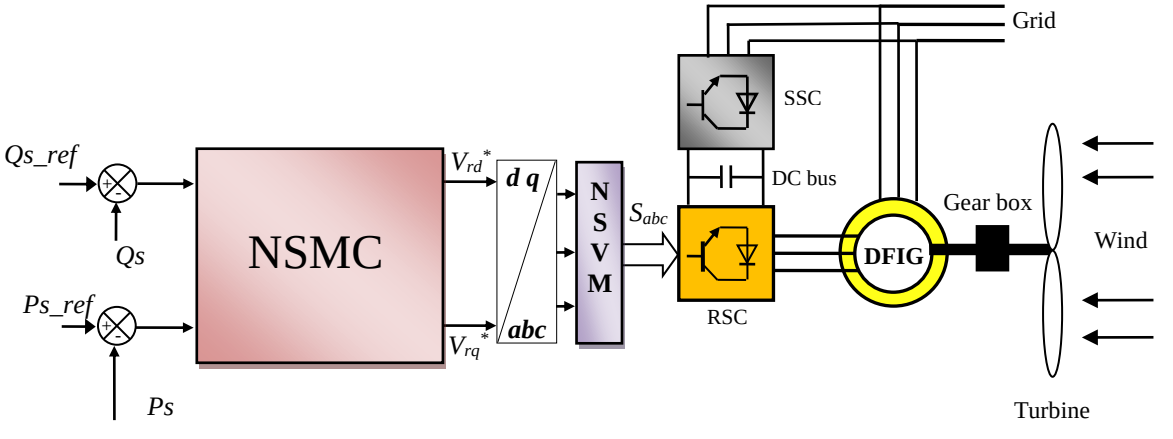

Fig. 11. NSMC control of a DFIG using NSVM strategy.

7.1. Reference tracking test

The objective of this test is the study of the two command schemes (SMC-3L-SVM and NSMC-3L-NSVM) behaviour in reference tracking. The simulation results are presented in Figs 12-19. As it's shown by Figs. 14-16, for the two regulators, the stator active and reactive powers track almost perfectly their reference but with an important response time for the classical SMC-3L-SVM regulator compared by NSMC-3L-NSVM technique. Therefore it can be considered that the two proposed types of SMC's have a very good performance for this test. On the other hand, Figs. 12-13 shows the harmonic spectrum of the one phase of rotor current. Table 3 shows the comparative analysis of THD value. See Table the THD value is significantly reduced when the NSMC-3L-NSVM is in use. Figs. 17-19 shows the zoom in the stator active power, stator reactive power and torque respectfully.

Table 3. Comparative analysis of THD value.

	THD (%)	
	SMC-3L-SVM	**NSMC-3L-NSVM**
Rotor current	0.33	**0.15**

These figures show that the ripple of stator active, stator reactive powers and electromagnetic torque in

the NSMC-3L-NSVM command scheme has been reduced compared to the classical SMC-3L-SVM command.

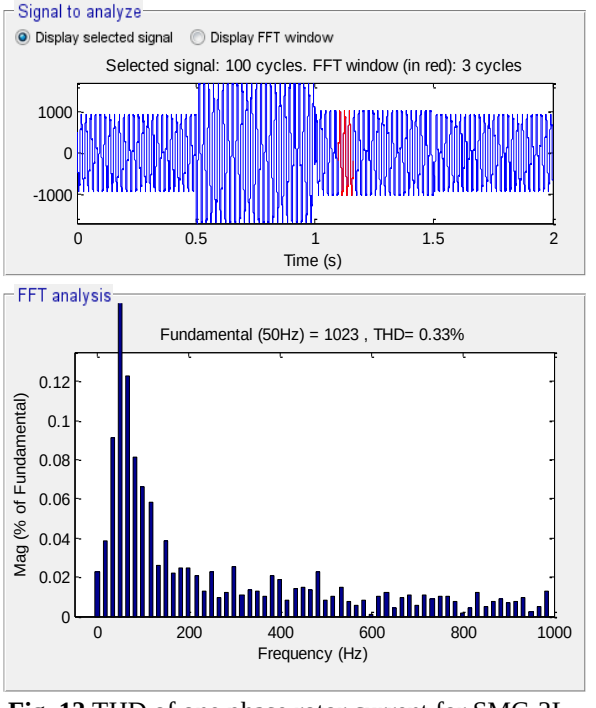

Fig. 12.THD of one phase rotor current for SMC-3L-SVM control (RTT).

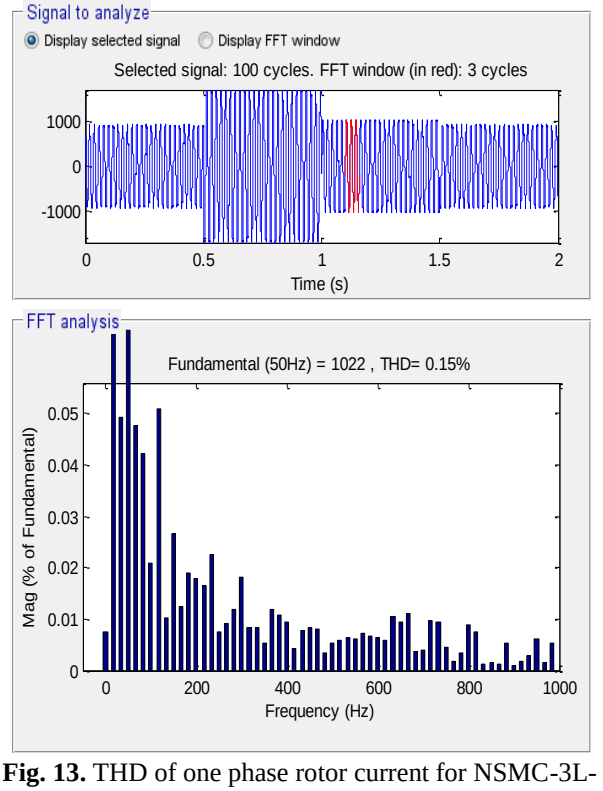

Fig. 13. THD of one phase rotor current for NSMC-3L-NSVM control (RTT).

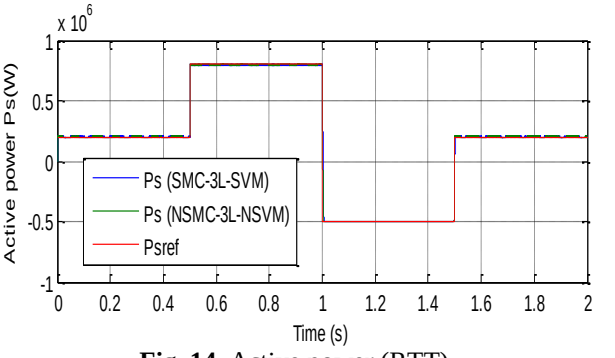

Fig. 14. Active power (RTT).

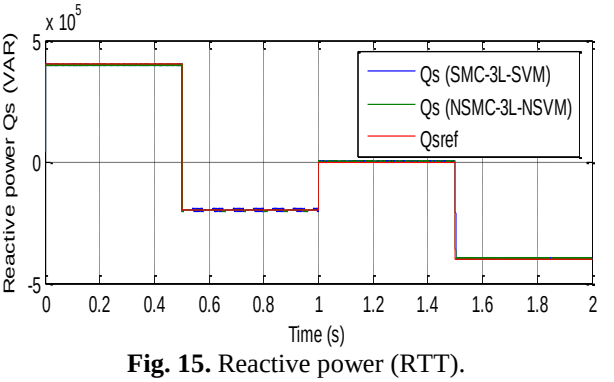

Fig. 15. Reactive power (RTT).

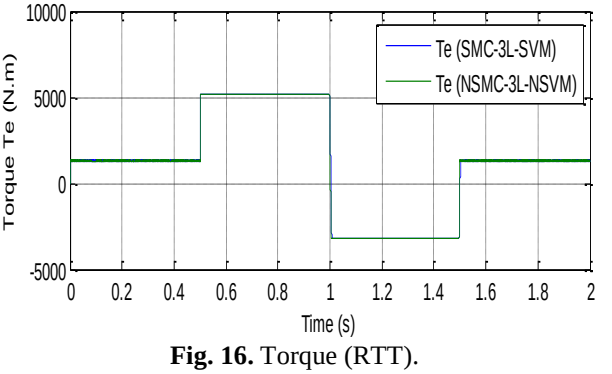

Fig. 16. Torque (RTT).

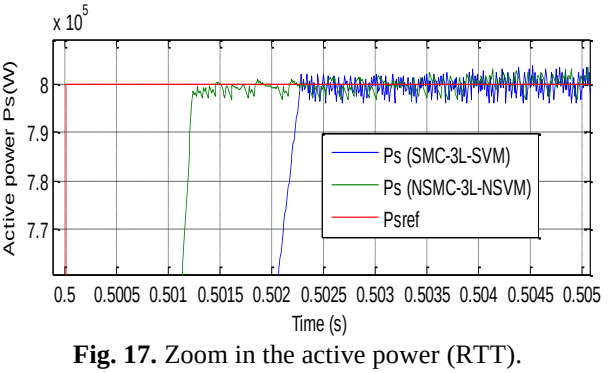

Fig. 17. Zoom in the active power (RTT).

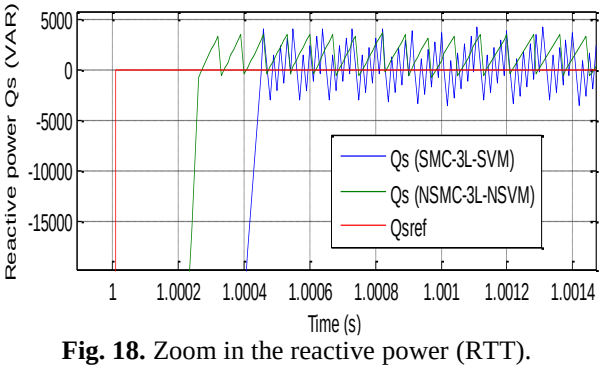

Fig. 18. Zoom in the reactive power (RTT).

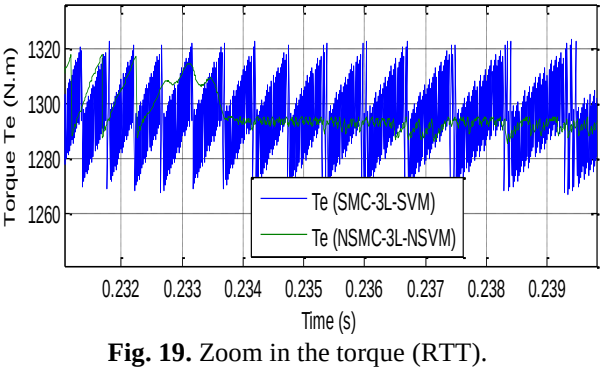

Fig. 19. Zoom in the torque (RTT).

7.2. Robustness Test

In order to test the robustness of the used regulators, the DFIG parameters have been intentionally modified with overkill variations : the value of the Rr and Rs are doubled, and the value of Lr, Ls and M are divided by 2. The gotten results are represented on Figs. 20-27. Figs.20-24 show the SMC-3L-SVM and NSMC-3L-NSVM strategy responses. Figs. 20-21 shows the harmonic spectrum of the one phase of rotor current. Table 4 shows the comparative analysis of THD value. Figs. 25-27 shows the zoom in the stator active, stator reactive power and electromagnetic torque respectfully. Table 4 and Figs. 25-27 shows that the NSMC-3L-NSVM command scheme is more and more robust compared to the traditional SMC-3L-NSVM command.

Table 4. Comparative analysis of THD value (RT)

	THD (%)	
	SMC-3L-SVM	**NSMC-3L-NSVM**
Rotor current	0.64	**0.37**

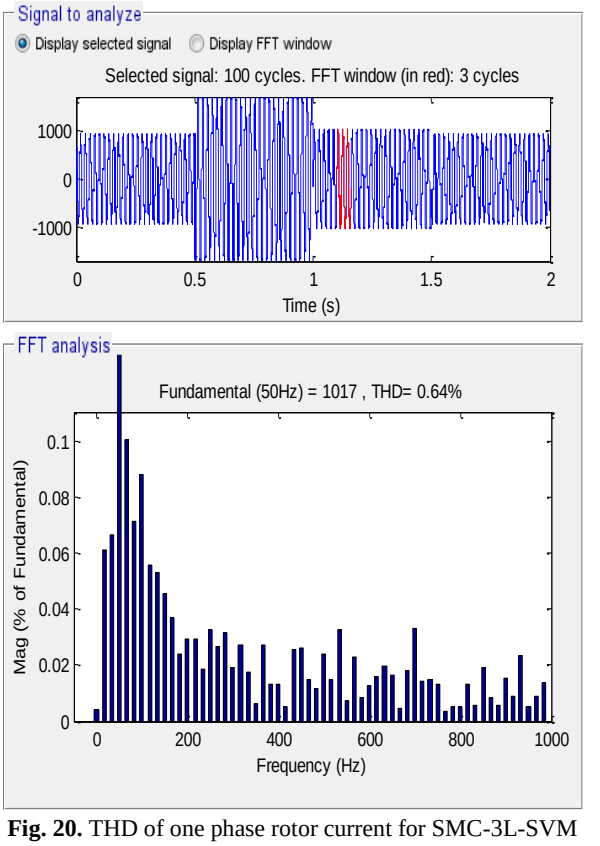

Fig. 20. THD of one phase rotor current for SMC-3L-SVM control (RT).

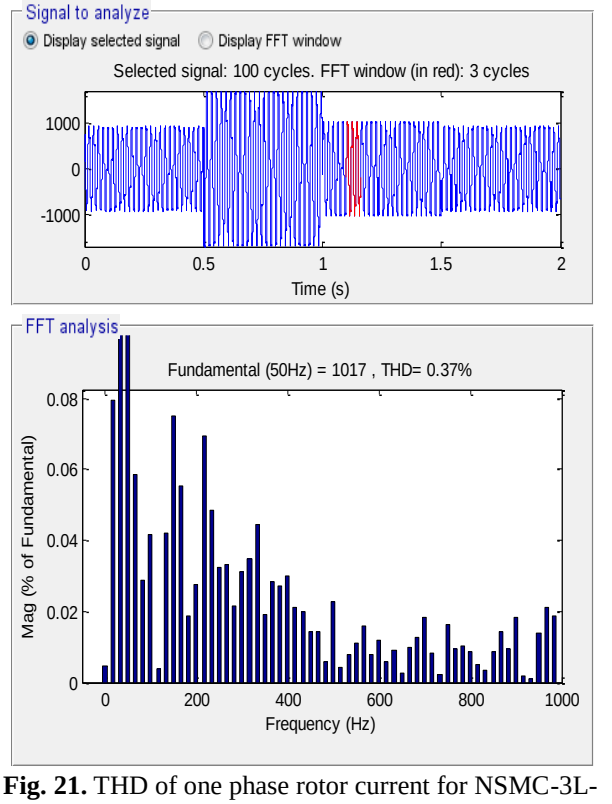

Fig. 21. THD of one phase rotor current for NSMC-3L-NSVM control (RT).

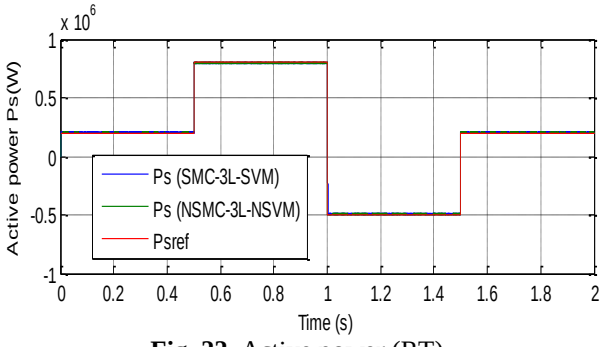

Fig. 22. Active power (RT).

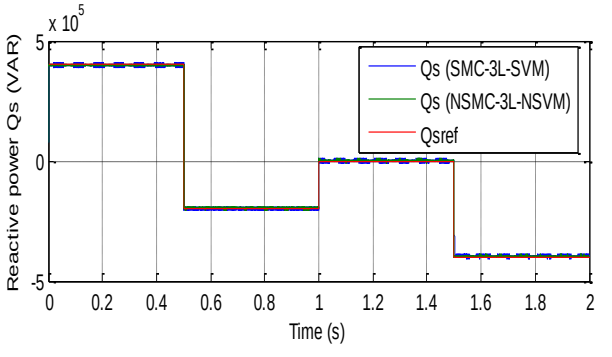

Fig. 23. Reactive power (RT).

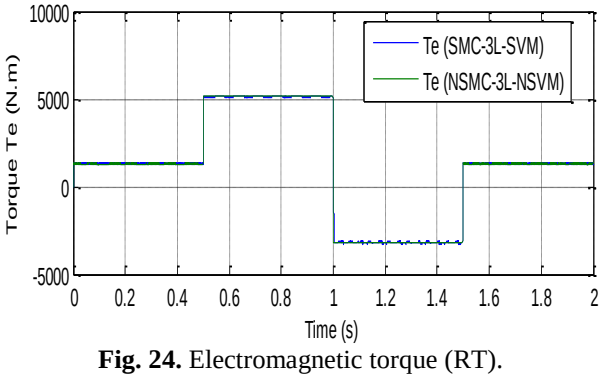

Fig. 24. Electromagnetic torque (RT).

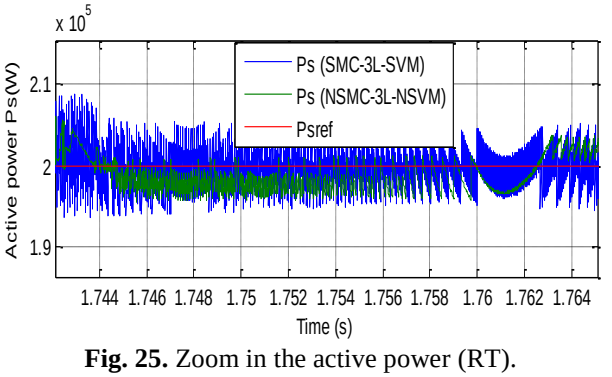

Fig. 25. Zoom in the active power (RT).

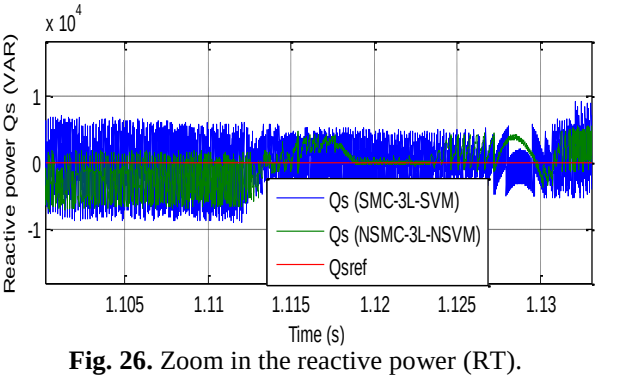

Fig. 26. Zoom in the reactive power (RT).

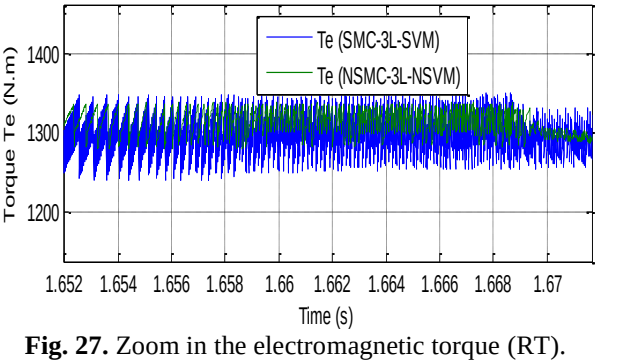

Fig. 27. Zoom in the electromagnetic torque (RT).

8. CONCLUSION

This work presents simulation results of NSMC for stator reactive and stator active power command of a DFIG for WT, using the 3L-NSVM inverter. With results obtained from simulation, it is clear that for the same operation condition, the DFIG stator reactive and active powers command with NSMC command using 3L-NSVM technique had better performance than the SMC command using 3L-SVM technique and that is clear in the spectrum of the stator reactive, stator active and phase rotor current harmonics which the use of the NSMC-3L-NSVM command scheme, it is reduced of harmonics more than classical SMC-3L-SVM command.

REFERENCE

[1] Z. Boudjema, R. Taleb, A. Yahdou, "**A new DTC scheme using second order sliding mode and fuzzy logic of a DFIG for wind turbine system**," *International Journal of Advanced Computer Science and Applications*, Vol. 7, No. 8, pp. 49-56, 2016.

[2] M. Benbouzid, B. Beltran, Y. Amirat, G. Yao, J. Han, "**Second-order sliding mode control for DFIG-based wind turbines fault ride-through capability enhancement**," *ISA. Transactions, Elsevier*, Vol. 53, No. 3, pp. 827-833, 2014.

[3] M. Hasni, Z. Mancer, S. Mekhtoub, S. Bacha, "**Parametric identification of the doubly fed induction machine,**" *Energie Procedia*, Vol. 18, pp. 177-186, 2012.

[4] Z. Boudjema, R. Taleb, Y. Djerriri, A. Yahdou, "**A novel direct torque control using second order continuous sliding mode of a doubly fed induction generator for a wind energy conversion system**," *Turkish Journal of Electrical Engineering & Computer Sciences*, Vol. 25, pp. 965-975, 2017.

[5] E. H. Dursun, A. Durdu, "**Speed control of a DC motor with variable load using sliding mode control**," *International Journal of Computer and Electrical Engineering*, Vol. 8, No. 3, pp. 219-226, 2016.

[6] Z. Boudjema, A. Meroufel, Y. Djerriri, E. Bounadja, "**Fuzzy sliding mode control of a doubly fed induction generator for wind energy conversion**," *Carpathian Journal of Electronic and Computer Engineering*, Vol. 6, No. 2, pp. 7-14, 2013.

[7] F. Benezzek, W. Bourbia, B. Bensaker, "**flatness based nonlinear sensorless control of induction motor system**," International Journal of Power Electronics and Drive System, Vol. 7, No. 1, pp. 265-278, 2016.

[8] E. Benyoussef, A. Meroufel, S. Barkat, "**Three-level DTC based on fuzzy logic and neural network of sensorless DSSM using extende kalman filter**," *International Journal of Power Electronics and Drive System*, Vol. 5, No. 4, pp. 453-463, 2015.

[9] A. Yahdou, B. Hemici, Z. Boudjema, "**Second order sliding mode control of a dual-rotor wind turbine system by employing a matrix converter**," *Journal of Electrical Engineering*, Vol. 16, No. 4, pp. 1-11, 2016.

[10] A. Medjber, A. Moualdia, A. Mellit, M. A. Guessoum, "**Comparative study between direct and indirect vector control applied to a wind turbine aquipped with a double-fed asynchronous machine Article**," *International Journal of Renewable Energy Research*, Vol. 3, No. 1, pp. 88-93, 2013.

[11] F. Senani, A. Rahab, H. Benalla, "**Modeling and control of active and reactive powers of wind conversion system in variable speed based on DFIG**," *Revue des Energies Renouvelables*, Vol. 18, No. 4, pp. 643-655, 2015.

[12] S. Manivannan, K. Senthilnathan, P. Selvabharathi, K. Rajalashmi, "**A comparative study of different approaches presents in two level space vector pulse width modulated three phase voltage source inverters**," *International Journal of Energing Engineering Research and Technology*, Vol. 2, No. 5, pp. 1-18, 2014.

[13] T. Sutikno, A. Jidin, M. F. Basar, "**Simple realization of 5-segment discontinuons SVPWM based on FPGA**," *International Journal of Computer and Electrical Engineering*, Vol. 2, No. 1, pp. 1793-8163, 2010.

[14] A. K. Bilhan, E. Akbal, "**Modeling and simulation of two-level space vector PWM inverter using photovoltaic cells as DC source**," *International Journal of Electronics, Mechanical and Mechatronics Engineering*, Vol. 2, No. 4, pp. 311-317, 2012.

[15] A. Idir, M. Kidouche, "**Direct torque control of three phase induction motor drive using fuzzy logic controllers for low torque ripple**," *Proceedings Engineering & Technology*, Vol. 2, pp. 78-83, 2013.

[16] M. Lešo, J. Žilková, M. Biroš, P. Talian, "**Survey of control methods for DC-DC converters**," *Acta Electrotechnica et Informatica*, Vol. 18, No. 3, pp. 41-46, 2018.

[17] B. Hamane, M. L. Doumbia, M. Bouhamida, A. Draou, H. Chaoui, M. Benghanem, "**Comparative study of PI, RST, Sliding mode and fuzzy supervisory controllers for DFIG based wind energy conversion system**," *International Journal of Renewable Energy Research*, Vol. 5, No. 4, pp. 1174-1184, 2015.

[18] Z. Boudjema, A. Meroufel, Y. Djerriri, "**Nonlinear control of a doubly fed induction generator for wind energy conversion**," *Carpathian Journal of Electronic and Computer Engineering*, Vol. 6, No. 1, pp. 28-35, 2013.

[19] B. Zinelaabidine, A. Meroufel, A. Amari, "**Robust control of a doubly fed induction generator (DFIG) fed by a direct AC-AC converter**," *Przegląd Elektrotechniczny*, Vol. 12, pp. 213-221, 2012.

[20] Y. Bekakra, D. Ben Attous, "**Comparison study between SVM and PWM inverter in sliding mode control of active and reactive power control of a DFIG for variable speed wind energy**," *International Journal of Renewable Energy Research*, Vol. 2, No. 3, pp. 471-476, 2012.